Searching for Extra-Terrestrial Intelligence with the Cherenkov Telescope Array

Sophia Baker
For the degree of MPhys in Physics
Supervisor: Prof. Paula Chadwick
Department of Physics, Durham University
Submitted: April 21, 2021

Abstract

We investigate the potential use of the Cherenkov Telescope Array (CTA) in the Optical Search for Extra-Terrestrial Intelligence (OSETI). An optimal list of 8 habitable exoplanet targets is selected via simple criteria: host stars must have a minimum age of 3 Gyr, so that intelligent life has had a chance to evolve, must generally be within 500 ly of Earth, and must fall within a 5° radius (approximately a CTA telescope's field of view) of possible subjects of CTA's planned Key Science Projects to allow for commensal observations. Assuming extra-terrestrial civilisations are transmitting pulsed, collimated signals towards Earth using laser technology possessed by humankind, OSETI is restricted to discrete wavelengths λ. CTA is sensitive to 300 nm $< \lambda <$ 550 nm. We investigate lasers with λ = 349 nm, 393.8 nm and 532.1 nm. We expect photon rates ranging from $\sim 10^{8}$ photons·ns^{-1} down to $\sim 10^{-1}$ photons·ns^{-1} for targets at distances 4.2 ly to 579 ly from Earth and transmitter diameters of up to 40 m. Signals exceeding the telescopes' Minimum Image Amplitudes (250 photons·ns^{-1} for SSTs, 400 photons·ns^{-1} for MSTs and LSTs) are possible from all 8 targets, hence OSETI is found to be feasible with CTA. However, as signal size is $\sim 10^{0}$ to $\sim 10^{2}$ milliarcseconds, we may require a single pixel trigger. Additionally, as the Maximum Routine Illuminations of CTA's PMT-utilising telescopes are up to 10^{4} times less than our greatest expected photon rates, damage to PMTs is possible. We discuss hardware modifications to alleviate this issue, as well as additional targeted observations during moontime, the potential for null results, statistical likelihood of signal detection, and the limitations of our methodology.

Despite caveats, we argue that OSETI with CTA is an endeavour worth undertaking. This project would not dramatically hinder existing projects, and, if successful, would be groundbreaking.

Contents

1 Introduction **3**
1.1 The Optical Search for Extraterrestrial Intelligence 3
1.2 The Cherenkov Telescope Array 4

2 Target Selection **6**
2.1 Choosing a Catalogue 6
2.1.1 The Catalog of Habitable Stellar Systems (HabCat) 6
2.1.2 The Habitable Exoplanet Catalogue (HEC) 7
2.2 Screening HEC for Targets 8

3 Transmission Schemes **11**
3.1 Technological Considerations 11
3.2 Photons Received 11
3.2.1 Derivation of Initial Expression 11
3.2.2 Modifications to Expression 13

4 Results **15**
4.1 Signal Size 15
4.2 Photon Rates 16
4.2.1 Proxima Cen b 16
4.2.2 Ross 128 b 19
4.2.3 GJ 1061 c and d 19
4.2.4 Teegarden's Star b and c 19
4.2.5 LHS 1140 b 20
4.2.6 Kepler-186 f 20
4.3 Interpretation of Results 20

5 Additional Targets **22**
5.1 Requesting Observing Time 22
5.1.1 Moonlight, Twilight and Dawn 22
5.1.2 Targeted Observations and TRAPPIST-1 23
5.1.3 "Empty" Regions of Sky and Serendipitous Observations 24

6 Further Discussion **24**
6.1 Improvements to Transmission Scheme 24
6.1.1 Limitations and Assumptions 24
6.1.2 Possibility of Incorrect Hypothesis 25
6.2 Habitability Revisited 25
6.3 Statistical Likelihood of Signal Detection 26

7 Conclusions **27**

1. Introduction

1.1 The Optical Search for Extraterrestrial Intelligence

Humankind's fascination with life beyond Earth is not new. Though the Search for Extra-Terrestrial Intelligence (SETI)[1] has only been active since 1959 [1], the "plurality of worlds" was the subject of speculation as long ago as ancient Greece, with Democritus alluding to life beyond Earth in the 4th century BCE [2]. By the end of the 17th century, with theological restrictions easing, the existence and nature of intelligent extra-terrestrial life (ET) had been postulated in popular scientific literature with Bernard de Fontenelle's *Conversations on the Plurality of Worlds*. Following soon after, Christiaan Huygens' *Cosmotheoros* provided a highly detailed hypothesis of the nature of life on other worlds and factors influencing said worlds' habitability [2–4].

It goes without saying that dramatic scientific progress has been made over the past three centuries, but even in the short time since the onset of SETI, there have been significant leaps in our knowledge and understanding of the universe. With the discovery of the first exoplanets, followed by the recent boom in their detection and characterisation, the number of known potentially habitable worlds is ever increasing; as of October 2020, NASA's Exoplanet Archive lists 4,296 confirmed planets [5].

The advancement of laser technology has also opened new doors in SETI, which has long revolved around radio signals [1, 6]. The Optical Search for Extra-terrestrial Intelligence (OSETI) centres on the hypothesis that ET communicates via collimated, narrow-band pulses of electromagnetic radiation provided by high-power lasers [7]. Such a pulsed signal, though mere nanoseconds (ns) in duration, could be visible as a point source outshining ET's host star in the night sky, with Howard et al. [8] stating that a pulsed laser signal originating 1000 ly away could appear a factor of 10^4 brighter than the communicating civilisation's host star.

There are multiple reasons for choosing ns pulses for interstellar communications. A signal on this timescale is immediately distinctive, as there are very few natural ns duration phenomena. It is also more cost-effective and energy efficient to produce a short, powerful laser pulse than it is to continuously emit light at the intensity required to cover interstellar distances. Less powerful continuous laser signals may be detectable as anomalies in the spectra of stars, but this method of detection requires that the SETI candidate star is similar to a star of known spectrum such that the spectra can be compared and anomalies caused by ET signals picked up on [7]. However, despite exciting hypotheses such as these, previous searches have not received any confirmed communications, optical or otherwise, from ET. This apparent silence is the subject of the Fermi Paradox [9]: why, if the universe is infinitely large, have we not detected, or been detected by, ET? Is anyone actually out there?

When faced with our apparent lack of company, it is important to acknowledge that in OSETI, null results do not rule out further investigation. Silence at a given time does not necessarily mean we are alone; it is possible to repeat observations of the same

[1]Note that in this work we use the abbreviations SETI and CETI to refer to the general search for extra-terrestrial intelligence and to communicating extra-terrestrial intelligence, not any particular organisation, e.g. the SETI Institute, unless otherwise specified.

target multiple times over an extended period and obtain different results each time, e.g. if the civilisation starts transmitting in the interim between observations. Aspects of the observation process may be changed between attempts, e.g. increased dwell time on target, or improvements in instrumentation. A change as small as this could be the difference between success and a null result [6].

Earth may be the intended recipient of pulsed optical communications, or our Solar System may, by pure chance, be positioned between an extra-terrestrial civilisation and whomever they are attempting to communicate with. Monte Carlo Realisation simulations tell us that if Earth is not the intended recipient, the interception of a collimated signal is unlikely, with a large signal opening angle (> 0.1 radians) required for such an event to be feasible [7]. However, the method used for these simulations has its limitations. Assumptions are made and key factors not considered; it is assumed that a constant number of civilisations exist for the full time over which the simulation is run, that all civilisations only send signals to one other partner civilisation, and follow-up signals sent by civilisations who have intercepted a signal are not included. There is also assumed to be an annular Galactic Habitable Zone (GHZ)[2], within which the number density of civilisations is assumed to be constant [7].

Despite the low likelihood of intercepting a collimated signal, collimated signals directed specifically at Earth, uncollimated or isotropic signals transmitted to a wider area, or weakly collimated signals travelling between civilisations, potentially intended to be intercepted, can still be sought. In this work, we propose and investigate the potential detection of pulsed, collimated communication signals from ET, directed at Earth, by the new Cherenkov Telescope Array (CTA), discussing its features in the context of OSETI, and computing preliminary estimates of how many photons we might expect to detect from such a signal.

1.2 The Cherenkov Telescope Array

When gamma rays with energies greater than a few GeV interact with Earth's atmosphere, cascades of subatomic particles are produced. As these particles travel faster than the speed of light in air, flashes of Cherenkov light, analogous to a sonic boom, are produced. These faint flashes of blue light are fleeting phenomena of ns-timescale, and so despite showers covering diameters of the order of kilometres, this Cherenkov light is invisible to the naked eye [11].

In order to carry out gamma ray astronomy from the Earth's surface, telescopes have been developed for the specific purposes of detecting and imaging Cherenkov light. These Cherenkov telescopes' ability to detect such faint, short timescale phenomena lends them well to the observation of other ns events, and so they are a valuable asset in OSETI. Various searches for optical pulses as proposed in §1.1 have been carried out using Cherenkov telescopes. The Very Energetic Radiation Imaging Telescope Array System (VERITAS), a prominent array of Imaging Atmospheric Cherenkov Telescopes (IACTs), recently dedi-

[2]The GHZ is an area defined by the radial metallicity and stellar density of the galaxy; this first condition is set out on grounds that metallicity must be sufficiently high to facilitate the formation of advanced biology, e.g. intelligent life, and for there to be sufficient heavy metal for said intelligent life to develop the technological resources required for communication. The stellar density must be such that the probability of interference with life by supernovae and other is low [10].

cated observing time to the Breakthrough Listen Initiative, a large-scale, highly sensitive SETI effort that has been running since 2015 [12].

This is not the only way Cherenkov telescopes can contribute to OSETI. Archival observational data can be searched for signals too; this approach was used to retrospectively observe KIC 8462852, a star identified as an "exceptional target" for SETI observations due to its abnormal light curve, via archival VERITAS data [13] (the search presented no evidence of pulsed beams as sought by OSETI from the star [13]). Archival data from the Solar Tower Atmospheric Cherenkov Effect Experiment (STACEE) has also been searched for ns laser pulses (with none confirmed) [6].

It is important to recall, as mentioned in §1.1, that these null results do not rule out future OSETI projects. In fact, the silence we have experienced thus far could be, in part, the result of our own observational constraints. Fortunately, the completion of a new generation of IACTs is on the horizon. With construction having begun and the first prototypes functioning in test runs, CTA should be functional in 2025 [12]. This new array is no different to other Cherenkov telescopes in that although its main planned use is gamma ray astronomy, other applications are possible, including optical observations, and hence OSETI [14]. Current instruments such as VERITAS and STACEE have their limitations, but CTA will overcome many of these by virtue of its sheer size.

STACEE is not a purpose-built Cherenkov telescope and hence has no imaging capability. Though capable of imaging, VERITAS is composed only of four 12 m diameter telescopes and, as such is less powerful than CTA, which will boast Small, Medium and Large Size Telescopes (SSTs, MSTs and LSTs) of diameters 4 m, 12 m and 23 m respectively, allowing the detection of gamma photons of energies from 20 GeV to 300 TeV, with threshold energies of 25 GeV and 80 GeV for the LSTs and MSTs respectively, and the SSTs providing coverage of energies upwards of $\sim$5 TeV [14, 15]. CTA's range of telescope sizes provide 9°, 8° and 4.5° fields of view (FOV); VERITAS is restricted to 3.5° [12].

The LSTs will provide approximately 4 times the light collecting power of VERITAS' four 12m telescopes. CTA consists of over 100 telescopes, spread between its northern (CTA-N) and southern (CTA-S) sites. These telescopes provide coverage of the entire sky and amount to a total light collecting area of the order of 10,000 m^2 [14, 16]. This large detection area will give rise to a high photon rate, facilitating the observation of ns-timescale phenomena, including any potential ns optical pulses transmitted by ET. CTA will also provide improved noise rejection [12].

Though the single mirror LSTs and MSTs feature traditional photomultiplier tubes (PMTs), the SSTs and some of the MSTs, which are double-mirror design Schwarzchild-Couder telescopes (SCT), will employ silicon photomultipliers (SiPMs). These relatively novel light sensors are a better match to these telescopes' plate scales; they also provide higher photon detection efficiencies, with the caveat that their efficiency peaks at higher wavelength than that typical of Cherenkov light [17]. As CTA-N is unable to observe the Galactic centre, it is not equipped with all three telescope sizes; SSTs are not necessary for the observation of other regions [14]. We discuss detector specifications in more detail in §3, §4 and §5.

The improvements in surveying and monitoring capability brought about by CTA, along with its flexibility of operation and capacity for simultaneous observations of objects and fields, make it an ideal instrument for OSETI. It is our intention to carry out

a search for collimated, narrow-band pulses using CTA. Such that no specific observing time need be dedicated to this project, and to capitalise on the extended observing times allocated in gamma ray astronomy, targets for OSETI will be selected based in part on their apparent proximity to CTA's planned areas of observation, such that we can "piggyback" on confirmed future projects.

2. Target Selection

2.1 Choosing a Catalogue

Target selection for OSETI with CTA begins with consideration of existing studies of exoplanet habitability. It is the general consensus that the presence of liquid water indicates a planet may host life. The concept of a star's habitable zone (HZ) arises from this hypothesis. The HZ is defined as "the circumstellar region around a star where a terrestrial planet with a suitable atmosphere could host liquid water on its surface" [18], with the assumption being that as life on Earth relies on liquid water, life on other planets does too [18]. This region is bounded by the "water-loss" (inner) and "maximum greenhouse" (outer) limits [19]. We note that this definition of the HZ caters to current limitations in SETI techniques. At present, remote observations of exoplanet atmospheres are relied on, and so SETI is restricted to life existing on planetary surfaces rather than that subsurface (water in an exoplanet's atmosphere is a good indicator of the presence of surface life, whereas the same cannot be said for life flourishing deep underground) [18].

Two suitable catalogues of potential targets, each following on from this concept of liquid water HZs, are considered: the Catalog of Habitable Stellar Systems (HabCat) [20], and the Habitable Exoplanet Catalogue (HEC) [21].

2.1.1 The Catalog of Habitable Stellar Systems (HabCat)

Constructed via elimination of unsuitable stars based on various habitability criteria, The Catalog of Habitable Stellar Systems (HabCat), produced for the SETI institute's "Project Phoenix" [20], lists 17,129 nearby Sun-like stars potentially hosting hospitable planets ("Hab-Stars"). HabCat was predominantly compiled via analysis of the Hipparcos Catalgoue, supported by complementary data from other catalogs and consideration of theoretical factors [20].

Stars lacking estimates of luminosity and temperature, which were deemed essential information, with large uncertainties in parallax as a result of parallax values less than zero, or with quoted fractional parallax uncertainties exceeding 30%[1] were immediately rejected [20].

Continuous habitability over long periods of time is a key requirement for the evolution and technological development of intelligent life and civilisation. The requirement for a minimum stellar age of 3 Gyr was therefore introduced, with the further constraint that any exoplanets must remain in a constant HZ over these billions of years [20]. Whether an exoplanet can remain within the HZ depends the stability of its orbit. In systems home to multiple stars, limitations on where stable planetary orbits can persist are significant.

[1]This uncertainty corresponds to uncertainty in absolute visual magnitude, $M(v)$, of $^{+0.57}_{-0.77}$ mag, a range that still allows determination of whether a star lies on the main sequence [20].

It is for this reason that HabCat only includes systems with one or two resolved stars [20]. The evolution of intelligent life on Earth despite the Sun's 11 year cycle is proof that life can thrive around a star exhibiting slight variation; however, out of caution, variable stars are all eliminated, again due to the requirement for a constant HZ [20].

Stars are also screened by spectral type. Some spectral types will have been immediately discarded as their ages do not satisfy $\tau_{min} = 3$ Gyr; this limits the sample to low mass main sequence stars [20]. With the concept of a constant HZ in mind once again, "terminal age" is considered. As a star evolves, the HZ around it moves, rendering previously habitable exoplanets inhospitable. Stellar metallicity evolution models provide information on which spectral types are likely to provide a constant HZ; undesirable spectral types can then be removed [20].

HabCat does not eliminate on grounds of stellar UV emissions. Though UV is potentially deadly, due to ozone feedback cycles, high UV emission from a star should result in orbiting exoplanets with thicker ozone layers, offering protection to life on the surface. UV concerns are particularly relevant to M-type stars due to the distribution of their spectral energy output [20].

Despite conflicting habitability arguments, which will be discussed further in §6.2, K- and M-type stars are still an important stellar demographic and so are included in HabCat. M-stars make up 75% of all stars [22], and their long main sequence lifetime provides the long-term stability required for the formation of complex life [20].

HabCat also selects stars based on a lower limit in metallicity, below which there would not be enough heavy elements to build an Earth-mass planet during solar system formations. No upper limit was applied [20]. This lower limit is also important in the context of the requirement of sufficient metallicity for the development of communication technology [10].

2.1.2 The Habitable Exoplanet Catalogue (HEC)

HabCat lists potentially habitable stars, not confirmed exoplanets. We recognise that astronomical instrumentation and observational techniques have progressed in the 17 years since its publication. The aforementioned recent boom in exoplanet detection and characterisation has also enabled further refinement in the selection of SETI targets; we now have a better idea of which of the thousands of "Hab-Stars" have potential to host life, as we know which are orbited by exoplanets, and characteristics of these exoplanets. Whilst many of the criteria used to compile HabCat remain relevant, it is an older resource and it consequently would be prudent to seek out a more modern catalogue, restricting our search to known exoplanets rather than unconfirmed potential host stars. We turn to UPR Aricebo's HEC for this more up-to-date selection of objects.

Exoplanets are chosen for HEC if they have a radius between $0.5R_\oplus$ and $2.5R_\oplus$ or a minimum mass between $0.1M_\oplus$ and $10M_\oplus$ (with these upper limits used to include Mega-Earths and water-worlds, and to account for uncertainties in measured radius and mass), they orbit an F-, G-, K- or M-type star (for reasons as discussed in [20]), and they orbit within the host star's optimistic HZ [21]. The latter two of these criteria were also presented in HabCat [20].

The compilation of HEC is ongoing, with regular updates to include newly detected

habitable exoplanets. The 60-strong catalogue lists candidates in two categories: "Conservative" and "Optimistic". The Conservative sample includes the exoplanets deemed the best candidates for surface liquid water support and rockiness. These are those with radius and mass less than $1.5R_\oplus$ and $5M_\oplus$ respectively. The remaining exoplanets, which are more likely to be "mini-Neptunes" than rocky planets supporting liquid water, make up the Optimistic sample [21].

2.2 Screening HEC for Targets

We take the 60 planets given in HEC and refine this list by introducing further constraints. Though most of these are based on practical observational considerations, we also borrow criteria from HabCat to eliminate those exoplanets home to non-communicative or unintelligent life, as HEC only lists habitable planets, not necessarily those hosting intelligent life.

Stars that are too young for intelligent life to have evolved are not a suitable SETI candidates. With this in mind, HabCat was restricted via its 3 Gyr minimum age threshold. We follow HabCat's lead and introduce a minimum age threshold, τ_{min}, to HEC, which does not eliminate based on stellar age [21]. Consultation of additional literature aids in the determination of τ_{min}. Recent research suggests $\tau_{min} = 5$ Gyr for a star to host intelligent life [10]. This figure is based on the assumption that intelligent, communicating extraterrestrial life will have evolved over a time period similar to that over which life did on Earth (4.6 Gyr) [10]. Recognising that the value of τ_{min} is arbitrary, as it is not guaranteed that extra-terrestrial life will have evolved under this timeframe, we choose to eliminate HEC's younger members using HabCat's more optimistic $\tau_{min} = 3$ Gyr, as filtering via $\tau_{min} = 5$ Gyr, would eliminate 73.3% of HEC, whereas $\tau_{min} = 3$ Gyr only eliminates 46.7%.

We do not carry forward HabCat's limit on number of stars per system or on stellar activity. These were cautious criteria put into place before more in depth studies of exoplanets and habitable zones had been made.

With necessary eliminations made via habitability criteria, practical observational criteria must be considered. To allow for commensal use of planned CTA observing time, we select targets which appear within CTA telescopes' fields of view when pointed at objects and areas of interest. To this end, the coordinates of the remaining HEC exoplanets are compared to those of every gamma ray source listed in the TevCat [23] and 2FHL [24] catalogues, and to those of the regions covered by CTA's Galactic Plane Survey (GPS), which covers latitudes $-5^\circ < b < 5^\circ$, and Extra-Galactic Survey (EGS), which covers latitudes $b > 5^\circ$ and longitudes $-90^\circ < l < 90^\circ$ [14]. An exoplanet must lie within a 5° radius of a gamma source, or in the GPS/EGS region, to be retained. This radius is chosen so that targets are comfortably within the FOV of both the MSTs and SSTs, whilst still likely being picked up by the LSTs.

When comparing the positions of the HEC objects to those of potential CTA targets, potential targets for CTA's Dark Matter Search, such as dwarf galaxies, have been neglected, as have the extensive 3FGL and 4FGL catalogues. This is because, for this initial investigation, it is not necessary to gather more exoplanet targets than TevCat and 2FHL "collect" by themselves.

The proximity-based selection process reveals an initial list of 14 exoplanets with potential to host complex, intelligent life. However, there are further reasons to potentially eliminate candidates from the sample. Following the inverse square law, the closer a planet, the better the chance of signal detection, and hence we generally do not investigate planets with distances greater than 500 ly. It is on these grounds that the majority of the Kepler planets (see Figure 2.1) do not make the final cut. We do, however, retain Kepler-186 f (8), as it is the closest of this subset of planets to Earth, and has the least separation from its neighbouring potential CTA target of all the planets.

We select the planets given in Table 2.1 and Figure 2.1 due to their close apparent proximity to potential CTA targets and actual proximity to Earth. The majority of these planets fall within the FOV of all three sizes of CTA telescope, as demonstrated in Figure 2.1, with the exception of LHS 1140 b (7), GJ 1061 c (3) and GJ 1061 d (4), which fall outside of, or on the very edge of, the LSTs' 4.5° FOV. These planets' proximity to Earth, however, outweighs these disadvantages. This being said, there is a balance to be struck between distance and brightness of the star itself. Stars that are too bright will drown out an OSETI signal or cause PMTs to age (an issue when apparent magnitude, $m_\star(v)$, reaches ∼4). Fortunately our target stars are sufficiently dim that this is not an issue (see Table 2.1).

Planet		$m_\star(v)$	R / ly	**Separation** / °	**Potential CTA Target**
1	Proxima Cen b	11.13[a]	4.2	3.37	Kookaburra (Rabbit)
				3.07	Kookaburra (PWN)
				1.89	HESS J1427-608
				3.34	RCW 86
				3.41	2FHL J1443.2-6221e
				3.21	2FHL J1419.3-6047e
				-	EGS & GPS
2	Ross 128 b	11.3[b]	11	-	EGS
3	GJ 1061 c	15.26[c]	12	4.5	2FHL J0318.0-4414
4	GJ 1061 d				
5	Teegarden's Star b	15.13[d]	12	3.57	2FHL J0238.8+1631
6	Teegarden's Star c				
7	LHS 1140 b	14.18[e]	49	4.97	KUV 00311-1938
					2FHL J0033.6-1921
8	Kepler-186 f	15.29[f]	579	1.66	MAGIC J2001+435
					2FHL J2001.2+4352
				-	EGS

Table 2.1: Exoplanet targets selected from HEC [21] via automated comparison with TevCat [23], 2FHL [24] and regions covered in CTA's Galactic Plane Survey (GPS) and Extragalactic Survey (EGS) [14] followed by manual refinement. $m_\star(v)$ is the host star's apparent magnitude in the v-band; R refers to the distance of each planet from Earth [5], and "Separation" to the apparent distances between planets and potential CTA targets. More comprehensive target summaries follow in §4. [a]From Jao et al. (2013) [25]; [b]from Research Consortium On Nearby Stars (acessed 2021) [26], [c]from Scholz et al. (2000) [27], [d]from Lépine et al. (2013) [28], [e]from Dittmann et al. (2017) [22], [f]from Quintana et al. (2014) [29].

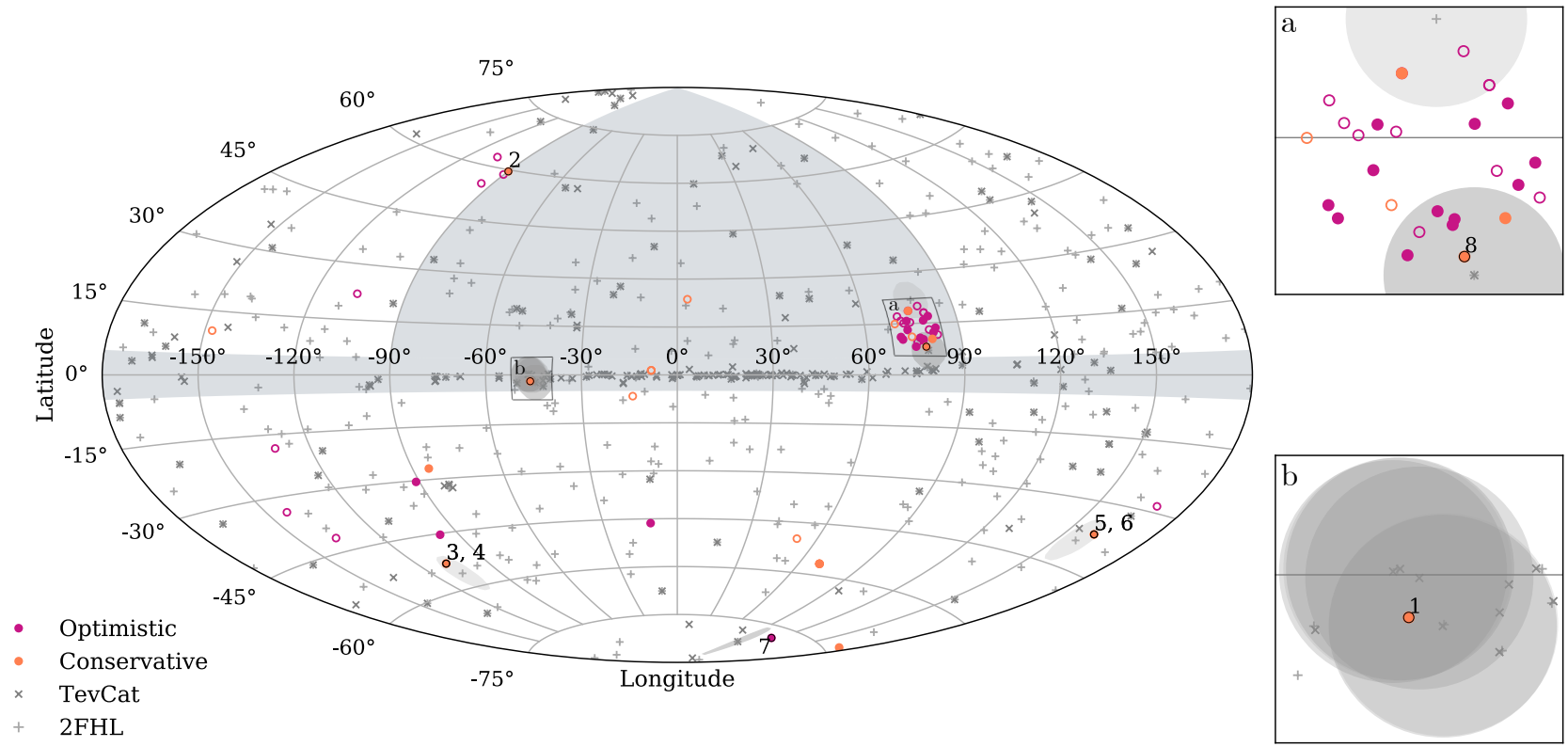

Figure 2.1: The positions of the HEC exoplanets [5] relative to known gamma ray emitting objects from the TevCat [23] and 2FHL catalogues [24] (with circular shaded regions of radius 5° placed around objects lying within 5° of said exoplanets) and the areas covered by GPS and EGS (represented by the larger shaded region; insets are left unshaded for clarity but show areas within the EGS). Exoplanets belonging to the Conservative and Optimistic catalogues are distinguishable by colour, with those eliminated on grounds of age represented by unfilled markers. Planets selected for manual evaluation are outlined in black and labeled with target ID numbers corresponding to the information given in Table 2.1. The cluster represented in inset region *a* is the group of exoplanets as detected by the Kepler mission, which solely took observations of this area of sky [30]. Inset region *b* shows the 6 potential CTA targets surrounding Proxima Cen b (1). This higher apparent density of gamma-ray objects is typical of the galactic plane. LHS 1140 b (7) appears outside of the shaded region around MAGIC J2001+435 due to the projection of the plot; as seen in Table 2.1, these objects are in fact within 5° of each other.

3. Transmission Schemes

3.1 Technological Considerations

The relationship between the wavelength, λ, and intensity of Cherenkov light scales as λ^{-2}, peaking in the blue-ultraviolet range, with data from La Palma showing a peak at ∼320 nm. The emission spectrum is bounded by atmospheric absorption below 300 nm. PMTs and SiPMs are sensitive to Cherenkov light's ∼300 nm $< \lambda <$ 600 nm range, and are fast enough to detect its ns flashes, hence will be utilised by CTA [31]. The Schwarzschild-Couder double mirror telescope design will compliment the SiPMs' small plate scale.

We will not search for pulses of $\lambda < 300$ nm, where atmospheric absorption occurs, and $\lambda > 550$ nm. Though Cherenkov light beyond this threshold is still emitted, its intensity has fallen by ∼50% by this point. In addition to this, strong emission lines corresponding to atomic oxygen, hydroxide and sodium occur at these higher λ [31]. Filters will be employed to block $\lambda > 550$ nm.

For the purpose of our preliminary computations, it is assumed ET has access to the same laser technology we do here on Earth. Tuneable lasers (e.g. the free electron laser) are inefficient and expensive, so are not considered [32]. This further restricts the pool of possible wavelengths for OSETI, as there are limited pulsable, high power lasers.

We considered restricting the search to green lasers, as these would be easily distinguishable from stars. However, CTA is most sensitive to blue light (as shown in Figure 3.2, PMTs are most efficient at ∼400 nm and SiPMs at ∼500 nm), and green lasers rarely meet criteria for power and pulsability, so this restriction is not applied.

Nd:YAG, with suitable lines for CTA at 532.1 nm (produced via 2nd harmonic generation) and 393.8 nm (produced via summed frequency generation), have been proposed as optimal lasers for transmission by ET [32, 33], and a full transmission scheme for the "Helios" laser, a diode-pumped Yb:S-FAP with potential to produce 3 ns pulses at $\lambda = 349$ nm with laser power, E_P, of 3.7 MJ is proposed in [8]. The "Helios" transmission scheme is a highly cited standard in OSETI publications; such a pulse has been predicted to appear 10^4 times brighter than its host star in our sky when pulsed from 1000 ly away [8].

If we assume ET is actively communicating with Earth, or looking to have signals intercepted, it is likely signals will preferably be transmitted at wavelengths that are likely to be observed, such as those of absorption lines in optical spectra. It is due to its proximity to the frequently observed CaK absorption line that the Nd:YAG's $\lambda = 393.8$ nm mode of operation is suggested [33]. Note that the power efficiency of this summed mode of operation has not been validated [32]. For both Nd:YAG-based transmission schemes, we assume $E_P = 2$ MJ and pulse length is 2 ns (based on [32, 33]).

3.2 Photons Received

3.2.1 Derivation of Initial Expression

The following derivation, as provided by [34], leads to an estimate of the number of photons, N_R, we expect a given telescope to receive per OSETI pulse of wavelength λ, originally formulated for the transmission scheme proposed in [8]. We will then modify

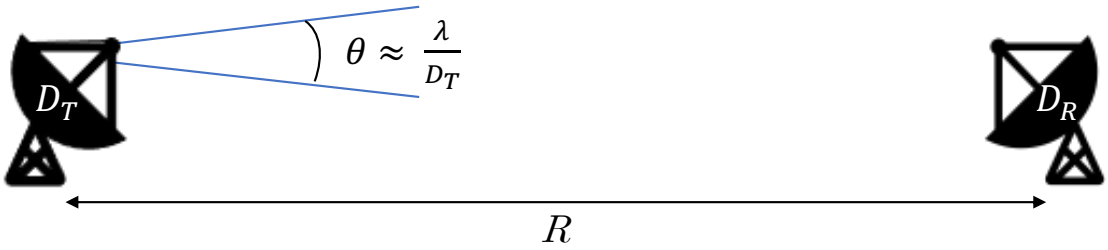

Figure 3.1: Diagram to aid in the derivation of Equation 3.9. D_T is the transmitter diameter, D_R the receiver diameter, R is their separation, and θ is the size of the transmitted laser beam.

this for the specific case of CTA. Initially, a simple version of the expression is derived, ignoring some factors of order unity. The derivation is then expanded upon to include these factors [34].

This transmission scheme assumes that a laser pulse of energy E_P and wavelength λ is beamed via an optical transmitter of diameter D_T to an optical receiver of diameter D_R over distance R (see Figure 3.1). With θ being the angular size of the pulsed beam [8,34],

$$\theta = \frac{\lambda}{D_T}. \tag{3.1}$$

The disc illuminated by the laser pulse at R has diameter θR. The fraction, F, of this disc received by a telescope of diameter D_R is hence found to be

$$F = \left(\frac{D_R}{\theta R}\right)^2. \tag{3.2}$$

The number of photons transmitted per pulse, N_P, can be given in terms of E_P, the pulse energy, as

$$N_P = \frac{E_p \lambda}{hc}. \tag{3.3}$$

Multiplying N_P (Equation 3.3) by the fraction of the pulse that will be received (Equation 3.2), and substituting Equation 3.1 for θ, leads to an expression for the number of photons received, N_R:

$$N_R = \frac{D_R^2 D_T^2 E_P \lambda}{\lambda^2 R^2 hc}. \tag{3.4}$$

We now account for the missing factors. The first of these is a correction factor for interstellar extinction, $10^{\frac{-2R}{5R_E}}$, where R_E is the distance over which a pulse will decrease in intensity by 1 mag, dependent on λ. For visible light, $R_E \approx 0.56$ kpc [35].

The next factor was not present in the simplified derivation as we should in fact have included the expression for the transmitter's "antenna gain", G_T, when giving the fraction of the pulse received. Assuming uniform illumination of the transmitter aperture,

$$G_T = 4\pi \frac{A_T}{\lambda^2}. \tag{3.5}$$

A_T and A_R are the areas of the transmitter and receiver respectively, i.e. (with $_i$ acting

as a placeholder for $_R$ and $_T$):

$$A_i = \pi \left(\frac{D_i}{2} \right). \tag{3.6}$$

Accounting for G_T leads to a new received pulse fraction,

$$F = G_T \frac{A_R}{4\pi R^2}, \tag{3.7}$$

into which Equations 3.5 and 3.6 are substituted, giving

$$F = \frac{\pi^2 {D_R}^2 {D_R}^2}{16\lambda R^2}. \tag{3.8}$$

We multiply N_P by this fraction, along with an interstellar extinction factor, to obtain the number of photons received at distance R, N_R:

$$N_R = \frac{\pi^2 {D_R}^2 {D_T}^2 E_p 10^{\frac{-2R}{5R_E}}}{16\lambda R^2 hc}, \tag{3.9}$$

as seen in [8]. As previously defined, N_R is the number of photons arriving at a telescope of diameter D_R, unbroadened, after travelling a distance R, beamed from a transmitter of diameter D_T. The interstellar extinction factor is $10^{\frac{-2R}{5R_E}}$. The energy of the laser pulse is E_p [8]; h is Planck's constant and c is the speed of light in a vacuum.

Counterintuitively, though more photons are emitted when a pulse of a given energy has a higher wavelength, and higher wavelengths are subject to less attenuation, N_R is inversely proportional to λ. Since we assume the beam is diffraction limited and hence described by Equation 3.1, lower λ radiation facilitates a broader beam and thus a greater number of received photons [8, 34].

3.2.2 Modifications to Expression

Equation 3.9 neglects atmospheric extinction. We must now consider its effects, described by the atmospheric extinction coefficient a_λ.

The value of a_λ varies between observing sites and with time, even over the relatively short duration of one night's observing. There is further variation dependent on the observed object's altitude, as an object at a larger zenith angle, z, will be obscured by more atmosphere, and so will be subject to more extinction than an object directly overhead. The relationship between an object's above-atmosphere magnitude, m_λ, and its magnitude at a given wavelength when viewed from the ground, $m_{\lambda,z}$, is given by [39]

$$m_\lambda = m_{\lambda,z} - a_\lambda(1 + \sec z). \tag{3.10}$$

The correction factor by which observational data must be multiplied to give unabsorbed above-atmosphere luminosity is [39]

$$k_{\lambda,z} = 10^{0.4 a_\lambda (1 + \sec z)}. \tag{3.11}$$

The inverse of this correction factor is applied to the quantity of unabsorbed photons

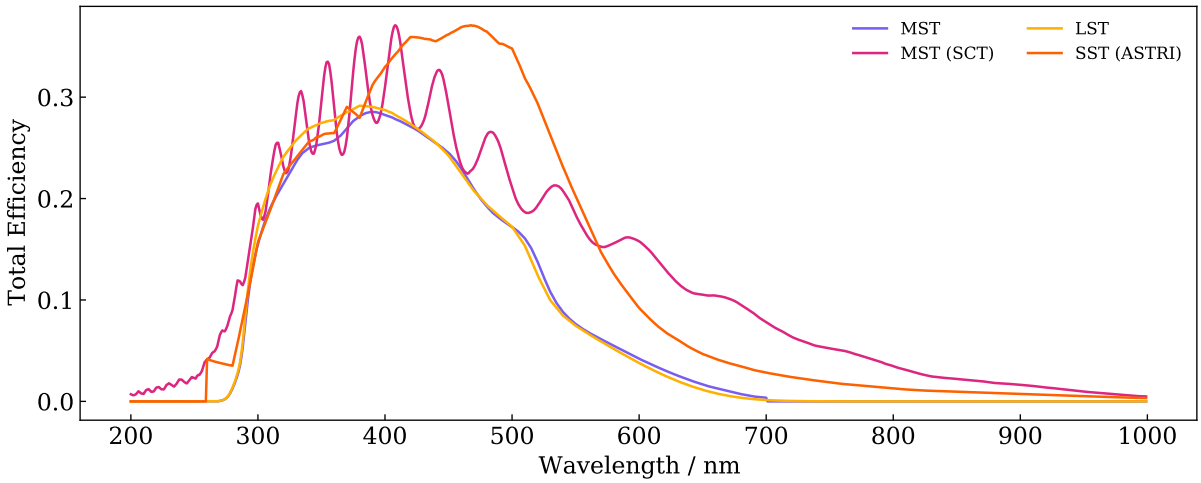

Figure 3.2: Each of the CTA Telescopes' simulated total efficiencies. Total efficiency is a combination of quantum efficiency, reflectivity, and the effects of the telescope's filter, funnel and masts. The SST (ASTRI) and MST (SCT)'s SiPMs lead to efficiency peaking at higher λ. Data via private communication with T. Armstrong (February 2021) [36].

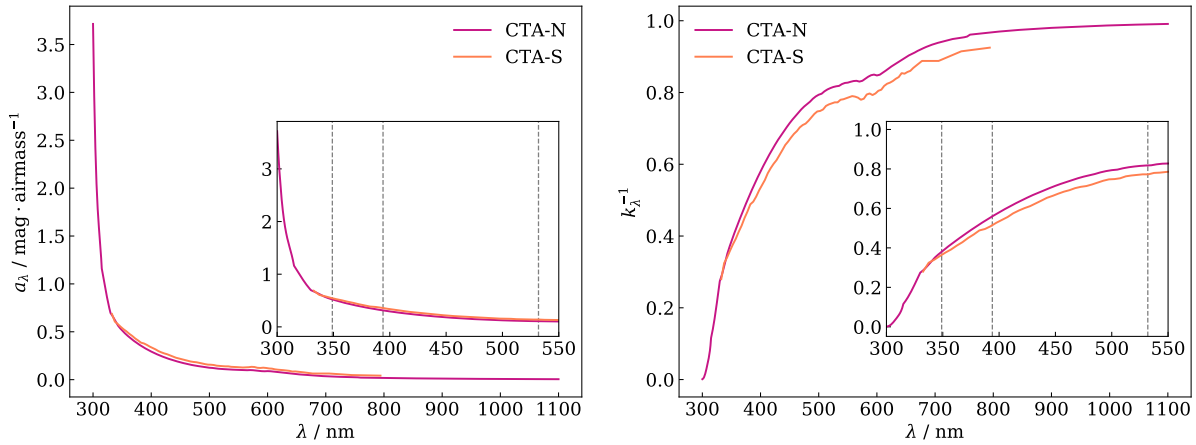

Figure 3.3: Computed values of a_λ (left) at Roque de los Muchachos Observatory (approximate location of CTA-N) and Cerro Paranal (approximate location of CTA-S) as calculated by King (1985) [37] and Patat et al (2011) [38] respectively and k_λ^{-1} (right) as calculated for each site via Equation 3.11. An arbitrary z of 10° is used here. Dotted lines mark λ of our chosen lasers. Insets show the λ of interest to CTA. Error bars are omitted for clarity; errors in a_λ are $\sim 10^{-4}$.

computed with Equation 3.9 to give the number of photons received at a given observing site after atmospheric absorption, our new N_R.

The receiving telescope's efficiency, η, is also neglected in Equation 3.9. The simulated relationship between η and λ is given in Figure 3.2 for each CTA telescope design [36]. We then find $\dot{N}_R$, the number of photons received per unit time in the case of a signal with transmitter of diameter D_{ET} detected by a CTA telescope of diameter D_{CTA} and efficiency η, to be:

$$\dot{N}_R = \frac{\eta}{k_{\lambda,z} t} \frac{\pi^2 {D_{CTA}}^2 {D_{ET}}^2 E_p 10^{\frac{-2R}{5R_E}}}{16 \lambda R^2 h c}. \tag{3.12}$$

	a_{349} / mag·airmass^{-1}	$a_{393.8}$ / mag·airmass^{-1}	$a_{532.1}$ / mag·airmass^{-1}
CTA-N	0.5208 ± 0.0001	0.3 ± 0.1 †	0.108 ± 0.001 †
CTA-S	0.5 ± 0.1 †	0.35 ± 0.01 †	0.139 ± 0.002 †

Table 3.1: Table of a_λ for each CTA site and laser, from data presented in Figure 3.3. We approximate values based on a_λ for λ closest to our desired values when a precise value is not calculated. Approximated values are annotated †.

We note that Equation 3.12 provides an estimate only. True interstellar extinction varies nonlinearly with distance and differs depending on direction. However, the R_E used here and in [8] does not correspond to the exact λ of the laser pulse, and instead is an average value for the visible portion of the electromagnetic spectrum.

The majority of CTA observations are carried out at low zenith angles, with the GPS and many other Key Science Projects (KSPs) requiring $z < 50°$ or $z < 45°$ [14]. With volume of atmosphere between observer and target, and hence atmospheric extinction, at a minimum directly overhead, we calculate $\dot{N}_R$ for observations of objects at their maximum possible zenith angle (assuming this is not less than ∼10°, as CTA's telescopes' mounts do not permit observations beyond this angle).

Atmospheric extinction will need to be specifically calculated at each CTA site for every night of observing [39]. With this CTA-specific data unavailable, literature values based on past observations local to the CTA sites are used. Calculated extinction curves for Roque de los Muchachos Observatory, La Palma (with which CTA-N will share a site) [37] and for Cerro Paranal, Chile (close to the site of CTA-S in altitude, latitude and longitude) [38] are plotted against λ in Figure 3.3, with relevant values in Table 3.1.

4. Results

4.1 Signal Size

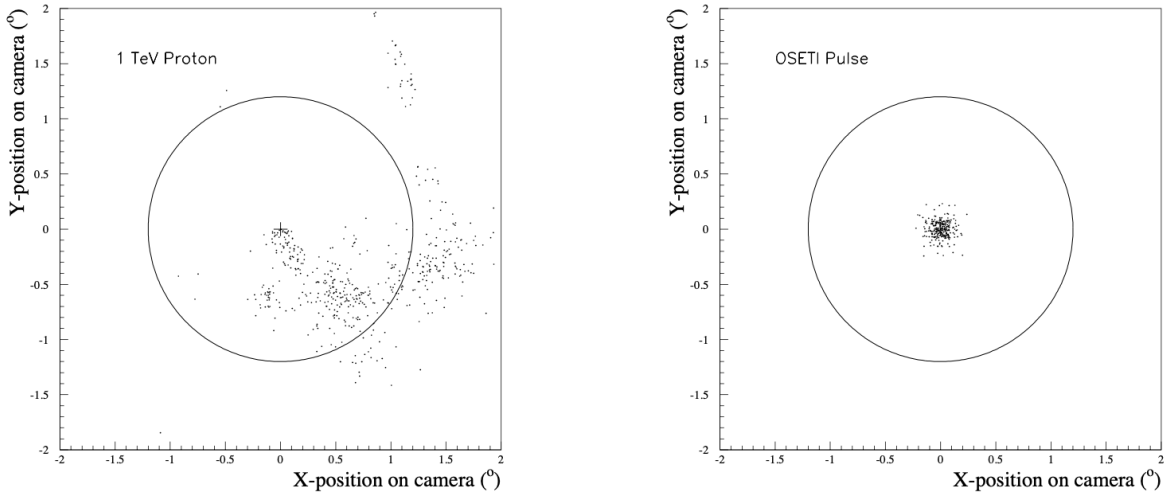

Figure 4.1: Figures by J. Holder et al. (2005) [40] demonstrating the difference in size and intensity between a simulated 1 TeV proton cascade (left) and an OSETI signal similar to, though less collimated than, those investigated in this work (right). The circle shows the FOV of the Whipple 10m telescope's camera.

Distant point sources such as laser pulses should be distinguishable from Cherenkov background and events as the latter have much greater angular size and ellipticity. A simulated example comparison is presented in Figure 4.1. Even low energy events, which trigger smaller showers, are distinguishable from point sources due to parallax, with images of Cherenkov showers subject to large displacements from camera to camera and OSETI signals appearing in the same location on each [13].
For all λ and D considered in our calculations, θ is to the order of 10 miliarcseconds Neglecting the effects of point spread function and seeing, this is a mere factor of $\sim 10^{-5}$ of the extent of a single pixel (the pixel pitches of the LSTs, MSTs and SSTs are 0.11°, 0.18° and 0.25° respectively) [36]. We therefore expect our signal to cover one pixel only. This leads to complications in that for standard observations, this will not meet trigger requirements. A new single pixel trigger will therefore need to be developed in future work.

4.2 Photon Rates

We now present, for each of the previously introduced targets and lasers, plots of photon rate, $\dot{N}_R$, against transmitter diameter, D_{ET}, as calculated for a best case observation (see Figures 4.2 and 4.3). Each planet's location in the sky, and hence its minimum zenith angle, is assessed to determine its visibility at each CTA site; we apply the visibility condition $z < 45^\circ$ [14]. $\dot{N}_R$ is then calculated for that minimum zenith angle, i.e. for the case of minimum atmospheric extinction. Errors in $\dot{N}_R$ are calculated via the functional approach described by [41]. Each telescope's Minimum Image Amplitude and Maximum Routine Illumination, as given in [36], is marked on its respective plots as "minimum threshold" and "saturation". These results are accompanied by a short profile of each target, further justifying its selection. The results' implications are discussed in §4.3.

We choose D_{ET} as our dependant variable as the other variable components of Equation 3.12 are better constrained (e.g. laser characteristics can only take discrete values, as can the distance travelled by the pulse given that we assume it originates from a target planet). $\dot{N}_R$ is computed for 1 m $< D_{ET} <$ 40 m. This upper bound is based on the size of the ELT, the world's largest telescope by diameter [42].

4.2.1 Proxima Cen b

Proxima Cen b is a promising target for OSETI. Not only is it certain to be observed by CTA-S thanks to its minimum zenith angle, position in the EGS & GPS regions and proximity to multiple objects, but it is orbiting *the* closest star to the Sun. Proxima Cen b has a suitable equilibrium temperature, $T_{eq} = (234^{+6}_{-14})$ K, for the presence of liquid water [43] and is a terrestrial planet of similar size to Earth, with mass $1.3 M_\oplus$. It is possible that the planet's possible tidal locking, though a controversial topic in habitability discussions, may actually be advantageous to life, as the strong magnetic fields of tidally locked planets offer the atmosphere protection from erosion via stellar magnetic fields and flares. This defence is much needed, as Proxima Centauri, an M5.5V-type star, has an average global magnetic flux (600 ± 150) times that of our Sun [43]. Figure 4.2 shows $\dot{N}_R$ from Proxima Cen b at CTA-S for a range of D_{ET}.

The Kookaburra, a pulsar wind nebula (PWN) complex, coincides with Proxima Cen b in the sky. The Kookaburra is likely to be included in CTA's investigation of Galactic

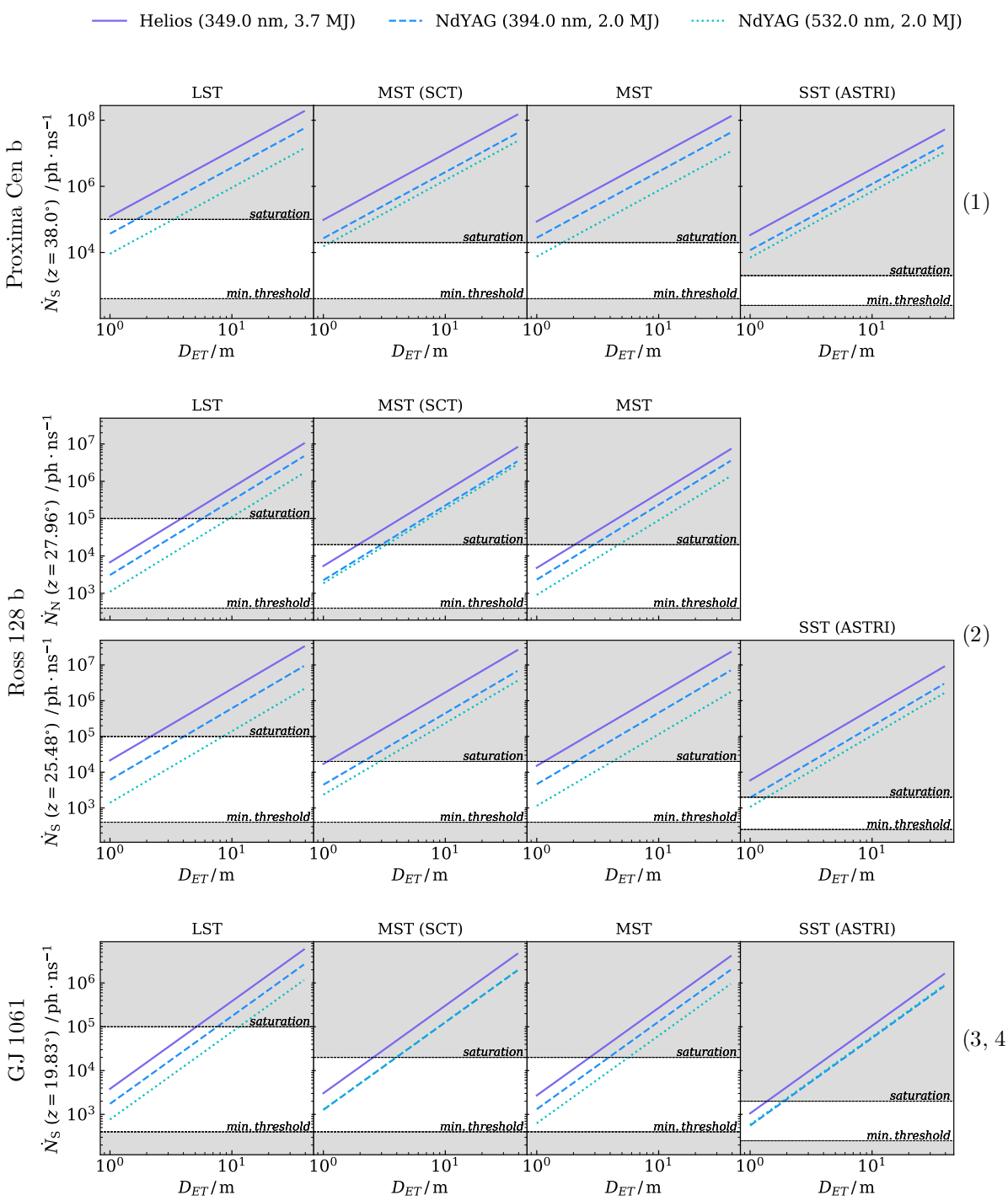

Figure 4.2: Plots of $\dot{N}_R$ vs D_{ET} for each CTA site, telescope design and potential laser, for each planet. Errors in $\dot{N}_R$ are of the orders of **(1)** 10^4 to 10^5, **(2)** 10^3 to 10^4 and **(3,4)** 10^3 to 10^4; they are not shown on these plots for clarity.

transients. Interest in PWNe as transients has been sparked by, among other things, the discovery of bright, high-energy gamma flares from the Crab nebula, as prior to this, PWNe had just been observed as steady sources. RCW 86, another of Proxima Cen b's neighbouring objects, is a supernova remnant and is possibly the most interesting object to CTA in this field [14]. 1020h of CTA's 1100-1300h/yr observing time has been requested of CTA-S for the GPS, which is expected to run for 10 years [14]; 780h of this is dedicated

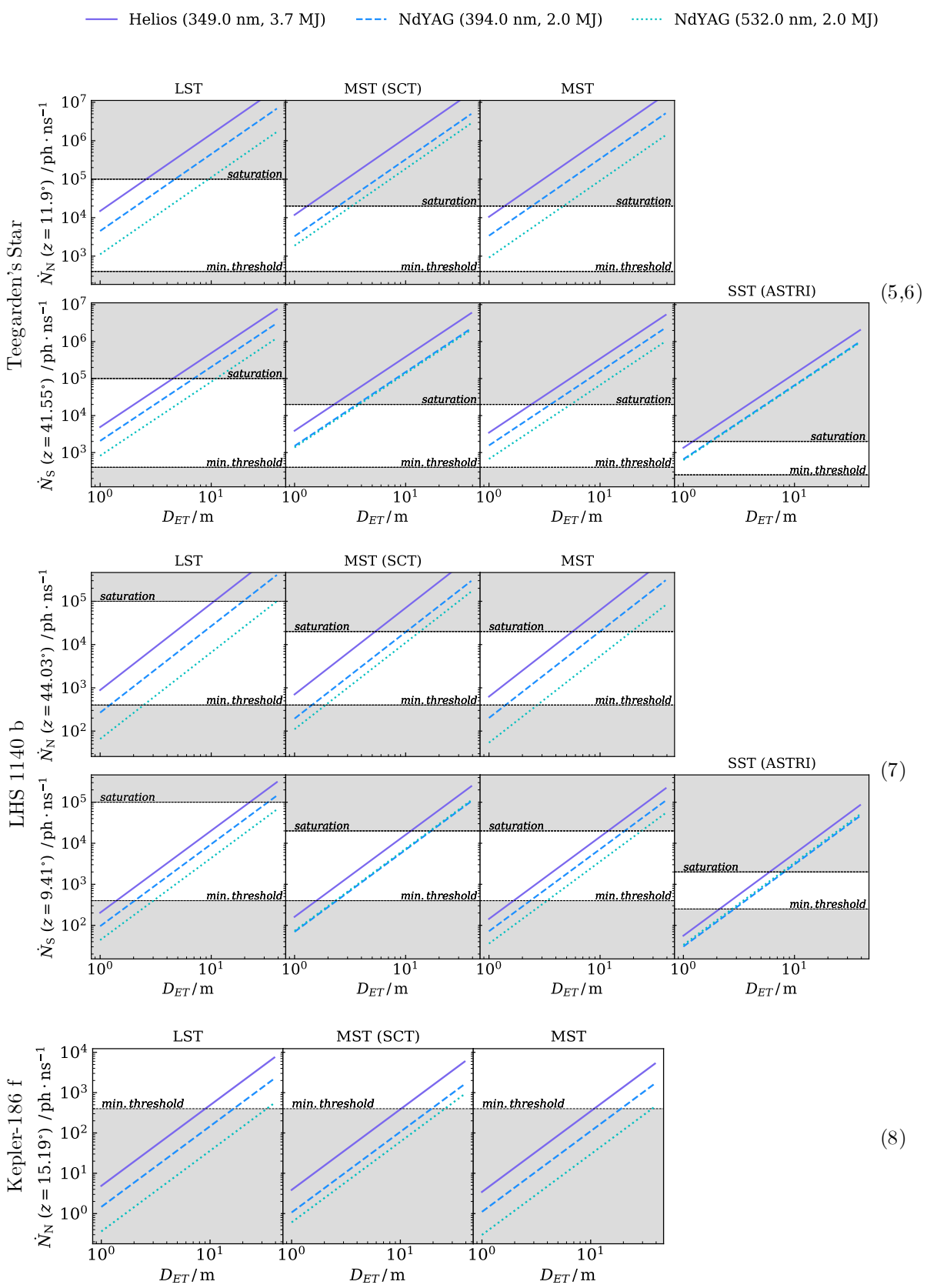

Figure 4.3: Plots as in Figure 4.2, now with errors in $\dot{N}_R$ of the orders of **(5,6)** 10^3 to 10^4, **(7)** 10^2 to 10^3 and **(8)** 10^0 to 10^1; they are not shown on these plots for clarity.

to the "inner region", where Proxima Cen b lies. If this time were to be shared equally over the "inner region", Proxima Cen b would receive ∼20h of observation. For context, VERITAS' observations for Breakthrough Listen are 15 minute intervals totalling at 30h/yr [12].

4.2.2 Ross 128 b

The second closest target to Earth after Proxima Cen b, and the second closest exo-Earth [44], Ross 128 b also falls in the range of the EGS region, though not in the proximity of any objects listed in the TevCat or 2FHL survey catalogues. Like Proxima Cen b, Ross 128 b orbits an M-dwarf. However, unlike the active Proxima Centauri, Ross 128, an M4-type star, has slow rotation and weak magnetic activity [44]. These factors are promising in the context of habitability, providing potential for atmospheric retention by the planet. Despite its placement close to the habitable zone's inner edge, Ross 128 b is thought to be cooler than Earth, with estimates suggesting 213 K $< T_{eq} <$ 269 K (based on the albedos of Venus and Earth respectively) [44]. Its close proximity to its host does, as with Proxima Cen b, raise questions of tidal locking.

Ross 128 b will be observed as part of the EGS, for which CTA-N will devote 600h to 10% of the sky, and CTA-S will devote 400h to 15% more. This will be over a period of up to 3 years [14]. How much of this time will be spent on Ross 128 b's surrounding area is unclear thus far. Figure 4.2 shows $\dot{N}_R$ for Ross 128 b at CTA-N and CTA-S for a range of D_{ET}.

4.2.3 GJ 1061 c and d

GJ 1061 is the 20$^{\text{th}}$ closest star to the Sun. Though sharing Proxima Centauri's spectral type, M5.5V, the star is relatively magnetically inactive and only emits low levels of X-ray radiation [45]. Lying comfortably in the liquid water habitable zone, the amount of energy received by GJ 1061 d is similar to that received by the Earth from the Sun [45]. GJ 1061 c is of similar mass to, and shares an Earth Similarity Index of 0.86 with, GJ 1061 d [21]. Figure 4.2 shows $\dot{N}_R$ for GJ 1061 at CTA-N and CTA-S for a range of D_{ET}.

GJ 1061 appears within a FOV of the quasar 2FHL J0318.0-4414, which is the brightest member of galaxy cluster ACO 3112 [46]. This object is not listed explicitly as a potential target in [14] but may still be of interest to CTA.

4.2.4 Teegarden's Star b and c

Members of a "remarkable" system [47], Teegarden's Star b and c are strong contenders for SETI. Both have minimum masses close to $M_\oplus$ and lie in the habitable zone. Although both planets are likely tidally locked [48], planet b receives similar stellar flux to Earth and as such has $T_{eq} \approx T_{eq,\oplus}$ [47]. The presence of liquid water has been deemed possible for both planets under a broad range of atmospheric models [48]. The system is approximately twice the age of our Solar System [5]. Other than occasional flares, Teegarden's Star generally exhibits low activity for its spectral type (M7.0 V), increasing chance of atmospheric survival, and is magnetically quiet for an M-dwarf [47].

These planets are particularly notable targets as, from 2044 until 2496, the Earth is due to be observable as a transiting planet from Teegarden's Star [47]. Such a transit observation could establish Earth as a habitable exoplanet target from the perspective of

"Teegardians", hence prompting the transmission of a collimated pulse towards our solar system. This scenario fits our hypothesis: we are investigating the feasibility of OSETI Signals directed towards Earth. Figure 4.3 shows $\dot{N}_R$ for Teegarden's Star at CTA-N and CTA-S for a range of D_{ET}.

Commensal observations of Teegarden's Star rely on CTA interest in 2FHL J0238.8+1631. As a BL Lacertae object (or blazar) [46], this gamma source may be observed as part of CTA's AGN-focussed KSP; however, it is not explicitly listed as a potential target in [14].

4.2.5 LHS 1140 b

LHS 1140 b is a rocky super Earth in orbit of another cool M-dwarf (an M4.5V-type star) [22]. It is likely LHS 1140 b did not always orbit within the liquid water habitable zone due to its host star's initial greater luminosity and higher proportion of UV emission. By 40 Myr after stellar formation, however, LHS 1140 b is thought to have entered the habitable zone, hence still spending $>\tau_{min}$ in this region [22]. The planet's atmosphere would also have initially been subject to higher levels of irradiance and ionising radiation. Despite this, the atmosphere may still have been retained thanks to LHS 1140 b's large surface gravity and low insolation [22].

LHS 1140 b's greater distance from Earth makes it the first of our targets from which a signal may not exceed the minimum photon threshold of any of the CTA telescopes, as demonstrated in Figure 4.3, which shows $\dot{N}_R$ for LHS 1140 b at CTA-N and CTA-S for a range of D_{ET}.

KUV 00311-1938, also known as 2FHL J0033.6-1921, lies within the same FOV as LHS 1140 b. CTA-S observations of this BL Lacertae object [46] amounting to 16h have been suggested as part of CTA's high-quality spectra observation programme, a sub-programme of the AGN-focussed KSP [14].

4.2.6 Kepler-186 f

Kepler-186 f's distance from Earth also proves problematic with regard to minimum photon threshold. As in the case of LHS 1140, the young Kepler-186, an M1-type dwarf star, would have exerted extreme UV flux on Kepler-186 f. Photo-evaporation hence likely stripped Kepler-186 f of any gaseous envelope (though there is a chance the planet has retained a thin H/He envelope) [49]. The planet is approximately Earth-sized (with radius 1.11 ± 0.14 $R_\oplus$) but as its composition is unknown, its mass cannot be precisely constrained [49]. Assuming it is able to retain an Earth-like atmosphere, Kepler-186 f would be able to sustain liquid water on its surface [49]. Figure 4.3 shows $\dot{N}_R$ for Kepler-186 f at CTA-N for a range of D_{ET}.

In addition to its position in the EGS region, the planet appears to neighbour MAGIC J2001+435, a gamma source corresponding to 2FHL J2001.2+4352, a BL Lacertae object [46], which may, though not listed in [14], be observed in the AGN KSP.

4.3 Interpretation of Results

With $\dot{N}_R$ now computed for a range of D_{ET} and R for all three proposed laser schemes and all 8 targets, we discuss the implications of these results in the context of instrumentation.

We notice that in the case of CTA-S, the general trend of $\dot{N}_R$ increasing with decreasing λ does not always hold for the MST (SCT) and SST (ASTRI) telescope designs. This is because there is variation in efficiencies and extinction coefficients between the different wavelengths and different telescope designs. The efficiencies of the MST (SCT) and SST (ASTRI) designs peak at higher λ than those of the the LST and classic MST (see Figure 3.2). This results in more received photons for wavelengths closer to this peak efficiency.

When z is smaller, and as such the effects of atmospheric extinction are lesser, one would expect a higher photon rate. However, in the case of LHS 1140 b, we see fewer photons at CTA-S, where the planet boasts $z_{min} = 9.41°$, than at CTA-N, where $z_{min} = 44.03°$. A possible explanation for this is that the atmospheric extinction at CTA-S is greater than at CTA-N. At higher wavelengths, this disparity increases (see Figure 3.3).

Closer targets (smaller R) and larger transmitter sizes (greater D_{ET}) initially appear ideal, as under these conditions $\dot{N}_R$ exceeds the Minimum Image Amplitudes (250 photons·ns^{-1} for SSTs, 400 photons·ns^{-1} for MSTs and LSTs) with ease. However, in these cases, $\dot{N}_R$ also frequently exceeds the telescopes' Maximum Routine Illumination (2000 photons·ns^{-1} for SSTs, 2×10^4 photons·ns^{-1} for MSTs and 10^5 photons·ns^{-1} for LSTs). As is evident in Figure 4.2, signals from Proxima Cen b, with possible $\dot{N}_R$ ranging from $\sim10^4$ photons·ns^{-1} to $\sim10^8$ photons·ns^{-1}, are highly likely to exceed every telescope designs' Maximum Routine Illumination. $\dot{N}_R$ from Ross 128 b, GJ 1061 c and d, and Teegarden's Star b and c may also exceed Maximum Routine Illumination, with possible $\dot{N}_R$ ranging from $\sim10^3$ photons·ns^{-1} to $\sim10^7$ photons·ns^{-1}, as shown in Figures 4.2 and 4.3.

For the SiPM-utilising MST (SCT) and SST designs, this will not be an issue. This is because, unlike PMTs, SiPMs do not suffer from ageing when exposed to bright light, and as a result can be used to observe bright sources without need for sensitivity-degrading hardware interventions [50]. However, the LST and single mirror MST designs utilise classic PMTs, to which over-saturation can be devastating. PMTs age according to the amount of charge collected by the anode, which increases with light intensity. The solution to this issue is to reduce the gain of the detector. The factor by which this is done must not be an arbitrary large factor, as the resultant performance degradation would be too great. Collection efficiency and time response would decrease, and signal-to-noise ratio would worsen, along with pulse-to-pulse gain fluctuations [51]. We discuss this further in the context of moonlight in §5.

A compromise must be struck between distance and signal intensity, as we do not wish to have to make hardware modifications to protect PMTs from the adverse effects of saturation, but equally need to observe targets where $\dot{N}_R$ exceeds the minimum threshold. Signals from more distant targets (larger R), such as LHS 1140 b and Kepler-186 f, are only detectable at larger transmitter sizes (greater D_{ET}) as $\dot{N}_R$ fails to meet the minimum threshold for detection, as shown in Figure 4.3. The solution to this issue is to reduce the detection threshold. However, doing so introduces noise.

Thus far we have only considered detection by individual telescopes, a vast underutilisation of CTA's capacity. This is because it is not known at this stage how many telescopes will be available, or how much flexibility we may have with trigger levels, given that the observations proposed are "piggyback" observations. It would initially intuitively seem that as each telescope has a minimum photon detection threshold, observations using a combination of telescopes would not provide any advantage in terms of detecting smaller

numbers of photons. However, as the minimum threshold is introduced to eliminate background noise, is actually the case that when multiple telescopes are used, threshold can be reduced, as multiple telescopes in different positions allow for the elimination of local noise. The minimum number of photons detectable is therefore lower when multiple telescopes are used in parallel as opposed to a single telescope, and hence maximum R can increase and minimum D_{ET} can decrease. Multiple telescope observations are a given for the GPS, where 80% of each array will be in use [14].

5. Additional Targets

5.1 Requesting Observing Time

With confidence in the feasibility of OSETI with CTA now secured, we propose extension beyond "piggyback" observations via the request of observing time specifically for OSETI.

When requesting observations we must be mindful to select targets which maximise our chances of success. We therefore propose CTA dedicates observations to exceptional targets only. An exceptional target must be included on HEC's "Conservative" list and is ideally at least old as our Solar System to increase chances of Earth-like civilisation having evolved. Observations allowing for the monitoring of multiple targets, e.g. those of systems hosting multiple habitable planets or targets that appear within the FOV of each other, are also favoured, as they provide a higher chance of detection in fewer observations. Based on our previous results, we also favour nearby planets (those within 100 ly of Earth).

Aware that CTA will be in high demand for KSPs and other gamma ray astronomy observations, we suggest observing time for OSETI be requested during quieter periods, such as during moon time, twilight and dawn.

5.1.1 Moonlight, Twilight and Dawn

Conditions unsuitable for CTA's usual observations, e.g. moonlight, twilight and dawn (CTA's KSPs predominantly require dark skies [14]), could still be suitable for OSETI observations, and at these times, specific observing time for particular targets could be requested. Operation of CTA under bright moonlight with reduced sensitivity has been suggested as a means of enhancing the efficiency of the observatory [40]. In addition to OSETI, intensity interferometry, optical communication with distant spacecraft, and observations of Kuiper-belt object occultations of stars and very rapid events from compact astrophysical sources are potentially possible during moon time [14].

Knowledge of specific telescope sensitivities, alongside predicted background and signal photon rates, allows determination of the suitability of these brighter conditions.

The intensity of direct moonlight increases with wavelength. Though at 350 nm, it is similar to that of the dark NSB, by 550 nm it is over twice as bright [50]. However, bright moonlight raises many of the same concerns as bright OSETI pulse detection, as introduced in §4. Though SiPMs are suitable for use in these conditions, PMTs will generally be aged too fast by high intensity light exposure and hence permanently damaged.

With hardware modifications, PMTs can be used during moonlight. Gain reduction is a common method for the facilitation of moonlight observations. In the case of

MAGIC, observations can be extended from a maximum brightness of $12\times\mathrm{NSB_{Dark}}$ up to $20\times\mathrm{NSB_{Dark}}$ when gain is reduced by a factor of 1.7, and up to $100\times\mathrm{NSB_{Dark}}$ with the use of UV-pass filters [51].

Changing gain levels should be fairly trivial for CTA due to the digital nature of modern telescopes and detectors. However, such modifications would introduce limitations to CTA's performance, such as poor signal-to-noise ratio and higher minimum analysis threshold [51]. Filters, if not already in use, would be an additional financial and logistical challenge and therefore unjustifiable for OSETI at this stage; for context, VERITAS's UV-bandpass filters require a three-person crew to install or uninstall, taking approximately 60 minutes [52].

Although moonlight would introduce the requirement for a higher minimum analysis threshold, a bright OSETI signal should still appear with sufficient contrast to the night sky background (NSB).

VERITAS' 15 min interval observations totalling at 30h per year could serve as a guide for the duration of targeted OSETI observations during moon time, twilight or dawn [12].

5.1.2 Targeted Observations and TRAPPIST-1

HEC's Conservative tier is assessed again to find systems that meet the required criteria for targeted observations. The majority of the systems not already selected in the first "piggyback" pass have unknown ages, are too young, or are too distant, but two initially promising systems emerge.

Tau Cet f appears to be a suitable candidate; the star meets our age criteria, and is just 12 ly from Earth. However, the planet itself orbits so close to the habitable zone's outer edge that it likely has a mean global surface temperature of 233 K. It would hence

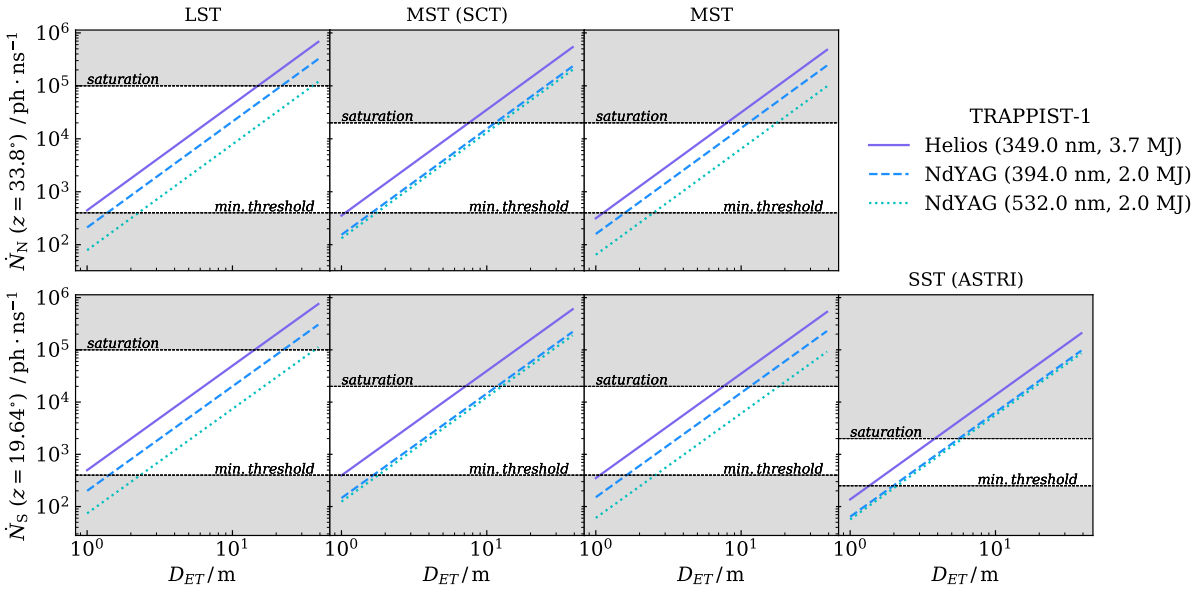

Figure 5.1: Plots of $\dot{N}_R$ vs D_{ET} for each CTA site, telescope design and potential laser for the case of TRAPPIST-1. Errors in $\dot{N}_R$ are $\sim 10^2$ to $\sim 10^3$ and are excluded for clarity.

only habitable to simple psychrophilic (cold-loving) life [53].

The TRAPPIST-1 system, however, perfectly fits our definition of an exceptional target. At only (12.14 ± 0.12) pc [54], or (39.60 ± 0.39) ly, from Earth, with an apparent v-band magnitude of (18.798 ± 0.082) [55], TRAPPIST-1 hosts four of HEC's "Conservative" habitable planets: TRAPPIST-1 d, e, f and g [21]. An ultracool, low-activity M8-type dwarf star [54], TRAPPIST-1 has been inferred to be (7.6 ± 2.2) Gyr old [56]. We note that although the lower limit of this figure, 5.4 Gyr, is in keeping with the evolutionary timescales of life as we know it, the upper limit, 9.8 Gyr, provides more scope for extinction events to have occurred, or even for technology to have developed beyond the laser pulses we seek. Figure 5.1 shows $\dot{N}_R$ as calculated for TRAPPIST-1 d, e, f and g for all λ and D_{ET} previously proposed.

5.1.3 "Empty" Regions of Sky and Serendipitous Observations

When areas of sky of less interest to gamma ray astronomers pass overhead, fewer observations will take up telescope time, presenting an opportunity for OSETI. We can flip the "piggyback" premise of target selection as described in §2 and request observations of targets in these regions as opposed to those close to known gamma ray objects or planned survey regions. Such observations could also serve as a blind gamma ray survey of the FOV surrounding the OSETI target, increasing chances of serendipitous gamma ray source discovery. However, a combined OSETI-gamma ray source observation would require far more observing time than the previously proposed 15 minutes, with ground based gamma ray observations requiring hours of uninterrupted observing time.

Serendipitous detection of OSETI signals is possible, with CTA's broader survey projects providing scope for such discoveries [14].

6. Further Discussion

6.1 Improvements to Transmission Scheme

6.1.1 Limitations and Assumptions

Aspects of our preliminary calculations could be refined. Interstellar extinctions specific to certain distances, wavelengths and Galactic coordinates, as opposed to an average visual band R_E, could be used in future calculations. Rather than approximating atmospheric extinction where values for a specific wavelength are unavailable, the a_λ-λ curve could be fitted with a function. This has not been done in this work due to the complex nature of the a_λ-λ relationship; a_λ includes many individual contributions (e.g. terms for Rayleigh scattering and aerosol contribution) [37].

Telescope integration time may require consideration as this is usually a few ns and we are investigating ns-timescale phenomena. However, assuming OSETI pulses of similar duration of a typical Cherenkov light flash, this should not be an issue.

We have not considered the atmospheric extinction a signal would suffer on the extraterrestrial end if transmitted from a ground-based instrument. We have also assumed signals will be transmitted from a planet itself, as opposed to from a travelling transmitter in interstellar space. We discuss limitations of our hypothesis further in §6.1.2.

We have assumed signals are brighter than night sky background without a full quantitative comparison, based on the statement that an OSETI signal from 1000 ly away could appear in the sky 10^4 times brighter than starlight [8].

6.1.2 Possibility of Incorrect Hypothesis

Even if ET is communicating in our vicinity, it is possible that they are not doing so via optical pulses with wavelengths in CTA's range of sensitivity. Our estimates of laser power and transmitter size could be too optimistic. Another consideration is collimation. This work hypothesises a collimated signal directed at Earth (or our Solar System). ET could instead be communicating via a broader beam in order to make contact with more potential civilisations, resulting in fewer received photons than we have calculated, or could not be communicating with Earth directly at all. It is unlikely that Earth would intersect a pulse beamed between two other civilisations unless the beam opening angle was to the order of 0.1 radians [7] (the signals simulated in this work have θ to the order of 10^0 to 10^2 milliarcseconds).

ET may not be communicating via the electromagnetic spectrum. An advanced civilisation could be transmitting messages using neutrino beams. This method of communication has been suggested not only as a means of interstellar and potentially intergalactic communication, but also for use as a means to contact deeply submerged submarines here on Earth [57–61].

It is assumed in this work that ET will attempt contact via existing Earth technology, neglecting the possibility that ET has developed tuneable pulsed lasers of sufficient efficiency and power for interstellar communication, providing access to a broader and more flexible range of laser wavelengths, energies and pulse lengths. In future work, hypothetical lasers could be investigated alongside transmission schemes based on humankind's current capabilities. ET might also communicate using means we are unable to comprehend or are yet to discover. However, we have confidence that extra-terrestrial life will have evolved to rely on the electromagnetic spectrum, just as we have here on Earth, and as such would be likely to utilise it not only as an energy source but as a means of communication. We can only hope that ET is broadcasting optically with the intention of having its signals intercepted.

6.2 Habitability Revisited

The targets selected in §2 may not be as habitable as assumed. We have not considered each planet's potential past exposure to catastrophic events such as supernovae or gamma ray bursts. A maximum age, τ_{max}, could also be considered, to account for stellar evolution interfering with the development of life, e.g. via runaway greenhouse heating. $\tau_{max} = 5.5$ Gyr suggested in [62] would eliminate GJ 1061 as a target system, as its age is estimated to be (7.0 ± 0.5) Gyr. The ages of other targets are either comfortably below 5.5 Gyr or subject to sufficient uncertainty that they may be less than 5.5 Gyr.

As exposed in the case of tau Ceti f, discussed in §5, minimum stellar age is not a failsafe condition for a planet's ability to host intelligent life. Other factors, such as surface temperature, metallicity and stellar mass should be considered if more comprehensively

screening targets. Host stars of masses below $0.10M_{\odot}$ can take several Gyr to contract onto the main sequence, which affects long term habitability of exoplanets [54].

Our targets are hosted by various M-dwarfs. The high levels of stellar activity typical of M-dwarfs is potentially problematic. However, this issue is not too prominent in the case of most of our targets, which are so-called "quiet" M-dwarfs. Of more concern is these stars' dimness. Although this is advantageous from an observational point of view (dim host stars allow for high contrast with OSETI signals and will not damage PMTs), the HZs of faint stars tend to be narrower and of smaller radii. Planets orbiting at such close proximity to their sun would be tidally locked [19].

A tidally locked planet would require a thick atmosphere to prevent atmospheric collapse [20] or transport heat to its dark side [19]. Thick atmospheres' potential interference with the stellar radiation required to reach a planet's surface could be very detrimental to the formation of life [20]. However, without the heat transfer provided by such an atmosphere, one side of the planet would remain permanently frozen and the other scorchingly hot, rendering the planet inhospitable to life as we know it. Despite this, the habitability of tidally locked planets has been argued for in many works [19].

We choose to have an optimistic outlook on M-dwarfs. Despite their potential drawbacks, M-dwarfs' slow luminosity evolution, which facilitates continuous habitable zones on Gyr timescales, is highly desirable when it comes to SETI [49]. These long-lasting habitability zones are another reason we neglect to restrict our targets, which are all M-dwarf systems, via any τ_{max}.

We were not, however, optimistic when comparing stellar ages to τ_{min}, not considering the minimum possible stellar age of a host implied by uncertainty in stellar age. There are therefore more potential targets that could be investigated in future work. The target list could also be expanded by considering planets appearing close to other CTA targets such as dwarf galaxies [14].

It is hypothesised that, if CETI are uniformly spread through the galaxy, our nearest CETI is 17000^{+33600}_{-10000} ly away [10]. If this is really the case, the search will yield a null result. However, there is no guarantee of this uniform spread of CETI; due to the GHZ, civilisations may well happen to exist in the same regions of the galaxy.

6.3 Statistical Likelihood of Signal Detection

The Breakthrough Listen Initiative recently detected a radio signal from the apparent direction of the Alpha Centauri system. However, it was rapidly ruled that this signal was not an ET technosignature or communication due to the low probability of the Alpha Centauri system hosting radio-transmitting ET ($\sim 10^{-8}$), as calculated under a framework determined by the Copernican principle [62]. The method used to calculate this probability is applicable to optical as well as radio SETI, and to other systems. Future work could investigate the probability of our target planets hosting optically communicating life via an adaptation of this method.

The Drake Equation could also be adapted to estimate our probability of detecting an OSETI signal. However, this method relies heavily on assumptions.

7. Conclusions

The Cherenkov Telescope Array, a new ground-based gamma ray observatory of unprecedented scale, provides a unique new opportunity for the Optical Search for Extra-Terrestrial Intelligence, the search for nanosecond optical pulses transmitted by extra-terrestrial civilisations. As CTA was designed specifically to detect ns-duration, optical Cherenkov light, it is also potentially suitable for OSETI observations.

We have assumed OSETI transmissions would originate from habitable exoplanets. Basing our target list on UCPR Arecibo's Habitable Exoplanet Catalogue [21], we imposed the additional criteria of a minimum stellar age, $\tau_{min} = 3$ Gyr, to discriminate between intelligent and unintelligent life (under the assumption that the former would take longer to evolve). So as to capitalise on the long observing times allocated to CTA's Key Science Projects, and to avoid the need to request additional observing time, we initially investigate the feasibility of commensal observations, proposing exoplanet targets that will appear within the field of view of a telescope when pointed at an area or object of interest to CTA. After elimination via these criteria and that of more distant planets, we were left with 8 target exoplanets.

Assuming extra-terrestrial civilisations have not advanced past current Earth technology, we selected possible pulsed laser transmission schemes. Only pulses of certain discrete powers and wavelengths are considered. With high power required to transmit over interstellar distances, and CTA's sensitivity only ranging from wavelengths of 300 nm to 550 nm, we were restricted to the "Helios" laser, a diode-pumped Yb:S-FAP operating at 349 nm and 3.7 MJ, and two modes of operation of the Nd:YAG laser at 532.1 nm (2nd harmonic generation) and 393.8 nm (summed frequency generation), both at 2 MJ.

The derivation of an expression for the expected received photon rate, $\dot{N}_R$, was then presented, modified from that for N_R as produced for Howard et al. [8, 34] to account for pulse length, telescope efficiency and atmospheric extinction. The minimum zenith angle, z, reachable by each exoplanet target at each of CTA's two sites, is calculated to determine whether said target will be observable by CTA (the KSPs generally require $z < 45°$, hence z outside of this range is assumed unobservable). $\dot{N}_R$ is then calculated for each planet when observed from the site(s) it will be visible from, for each proposed laser, for each of CTA's telescope designs (SST, MST, MST (SCT) and LST), and for transmitter diameters ranging from 1 m to 40 m.

With the very minimum detected photon rate calculated being $\sim 10^1$ photons·ns^{-1} for our most distant target (Kepler-186 f at distance 579 ly from Earth) and smallest transmitter diameter (1 m), we found that provided sufficient transmitter diameter, signals from all 8 targets could exceed the telescopes' Minimum Image Amplitudes (250 photons·ns^{-1} for SSTs, 400 photons·ns^{-1} for MSTs and LSTs). OSETI with CTA is consequently found to be a feasible endeavour.

However, there are caveats. Neglecting seeing and point spread function, signal size is of the order of milliarcseconds, introducing potential need for single pixel trigger development. For closer targets and larger transmitter sizes, damage to photomultiplier tube (PMT) based instrumentation is possible. For example, for a signal from Proxima Cen b, 4.2 ly away, $\dot{N}_R$ is of the order of up to 10^8 photons·ns^{-1}, surpassing the Maximum

Routine Illumination of the LSTs, which employ the ageing-prone PMTs, by a factor of 10^3. Permanent damage via ageing can be avoided by reducing detector gain, but this introduces performance limitations.

We also propose targeted observations of empty sky and the TRAPPIST-1 system during moon time under reduced gain conditions, for which observing time would be requested. Limitations and assumptions, in the context of both transmission schemes and target selection, were then discussed, as were possible statistical extensions to the project.

Although the low probability of detecting a message from an extra-terrestrial civilisation is low, and past searches have yielded only null results, we argue that Optical Search for Extra-Terrestrial Intelligence with CTA is worth undertaking. The scientific, philosophical and cultural impact of extra-terrestrial signal detection would be groundbreaking and would alter humankind's perspective of our place in the universe profoundly. With few negative implications for CTA, and a growing multitude of potentially habitable exoplanets, what is there to lose by trying?

References

[1] G. Cocconi and P. Morrison, "Searching for Interstellar Communications," *Nature*, vol. 184, no. 4690, pp. 844–846, 1959.

[2] S. Dick, *Plurality of Worlds*. Cambridge University Press, UK, 1984.

[3] H. Aldersey-Williams, *Dutch Light: Christiaan Huygens and the Making of Science in Europe*. Picador, UK, 2020.

[4] C. Huygens, *Cosmotheoros: Or Conjectures Concerning the Planetary Worlds, and Their Inhabitants*. Gale Ecco, Print Editions, USA, 2010 [originally 1698].

[5] *NASA Exoplanet Archive*. `https://exoplanetarchive.ipac.caltech.edu`, last accessed Jan 9, 2021.

[6] D. Hanna *et al.*, "OSETI with STACEE: A Search for Nanosecond Optical Transients from Nearby Stars," *Astrobiology*, vol. 9, no. 4, pp. 345–357, 2009. PMID: 19413506.

[7] D. H. Forgan, "Can Collimated Extraterrestrial Signals be Intercepted?," *JBIISs*, no. 67, pp. 232–236, 2014. arXiv:1410.7796.

[8] A. W. Howard *et al.*, "Search for Nanosecond Optical Pulses from Nearby Solar-Type Stars," *ApJ*, vol. 613, no. 2, pp. 1270–1284, 2004.

[9] E. Jones, "Where is everybody? An account of Fermi's question.," *Web.*, 1985.

[10] T. Westby and C. J. Conselice, "The Astrobiological Copernican Weak and Strong Limits for Intelligent Life," *ApJ*, vol. 896, no. 1, p. 58, 2020.

[11] *Centre for Advanced Instrumentation : Ground Based Gamma Ray Astronomy - Durham University*. URL: `https://www.dur.ac.uk/cfai/vhegammaraygroup/physics/groundbased/`, last accessed Apr 2021.

[12] V. Gajjar *et al.*, "The Breakthrough Listen Search for Extraterrestrial Intelligence," *arXiv e-prints*, 2019. arXiv:1907.05519.

[13] A. U. Abeysekara *et al.*, "A Search for Brief Optical Flashes Associated with the SETI Target KIC 8462852," *ApJ*, vol. 818, no. 2, p. L33, 2016.

[14] C. T. A. Consortium, "Science with the Cherenkov Telescope Array," 2018.

[15] H. Constantini and E. O. Angüner, "PeVatrons: The Hunt for the Origin of Galactic Cosmic Rays with CTA," *CTA Newsletter August 2020*, 2020.

[16] *How CTA will detect Cherenkov light*. URL: `https://www.cta-observatory.org/about/how-cta-works/`, last accessed Jan 9, 2021.

[17] M. Actis *et al.*, "Design concepts for the Cherenkov Telescope Array CTA: an advanced facility for ground-based high-energy gamma-ray astronomy," *ExA*, vol. 32, no. 3, pp. 193–316, 2011.

[18] A. Méndez *et al.*, "Habitability Models for Planetary Sciences," 2020.

[19] R. K. Kopparapu *et al.*, "Habitable Zones around Main-Sequence Stars: New Estimates," *ApJ*, vol. 765, no. 2, p. 131, 2013.

[20] M. C. Turnbull and J. C. Tarter, "Target Selection for SETI. I. A Catalog of Nearby Habitable Stellar Systems," *ApJS*, vol. 145, no. 1, pp. 181–198, 2003.

[21] "Planetary Habitability Laboratory @ UPR Arecibo." URL: `http://phl.upr.edu`, last accessed October 2020.

[22] J. A. Dittmann *et al.*, "A temperate rocky super-Earth transiting a nearby cool star," *Nature*, vol. 544, no. 7650, pp. 333–336, 2017.

[23] *TevCat 2.0*. URL: `http://tevcat2.uchicago.edu`, last accessed Jan 9, 2021.

[24] M. Ackermann *et al.*, "2FHL: The Second Catalog of Hard Fermi-LAT Sources," *ApJs*, vol. 222, no. 1, p. 5, 2016.

[25] W.-C. Jao *et al.*, "The Solar Neighborhood XXXI: Discovery of an Unusual Red+White Dwarf Binary at 25 Parsecs via Astrometry and UV Imaging," *ApJ*, vol. 147, no. 1, p. 21, 2013.

[26] *THE ONE HUNDRED NEAREST STAR SYSTEMS brought to you by RECONS (Research Consortium On Nearby Stars)*. URL: `http://www.recons.org/TOP100.posted.htm`, last accessed Mar 21, 2021.

[27] R. D. Scholz *et al.*, "New high-proper motion survey in the Southern sky," *A&A*, vol. 353, pp. 958–969, 2000.

[28] S. Lépine *et al.*, "A Spectroscopic Catalog of the Brightest (J<9) M Dwarfs in the Northern Sky," *AJ*, vol. 145, no. 4, p. 102, 2013.

[29] D. Souto *et al.*, "Chemical Abundances of M-Dwarfs from the Apogee Survey. I. The Exoplanet Hosting Stars Kepler-138 and Kepler-186," *ApJ*, vol. 835, no. 2, p. 239, 2017.

[30] W. Borucki *et al.*, "KEPLER: Search for Earth-Size Planets in the Habitable Zone," *Proceedings of the International Astronomical Union*, vol. 4, no. S253, pp. 289–299, 2008.

[31] A. Bouvier *et al.*, "Photosensor Characterization for the Cherenkov Telescope Array: Silicon Photomultiplier versus Multi-Anode Photomultiplier Tube," *Hard X-Ray, Gamma-Ray, and Neutron Detector Physics XV*, 2013.

[32] M. Hippke, "Interstellar communication: The colors of optical SETI," *JApA*, vol. 39, no. 6, p. 73, 2018.

[33] S.-y. Narusawa, T. Aota, and R. Kishimoto, "Which colors would extraterrestrial civilizations use to transmit signals?: The "magic wavelengths" for optical SETI," *New Astronomy*, vol. 60, pp. 61–64, 2018.

[34] P. Horowitz, "Derivation of Received Number of Photons." Private Communication, Mar 2021.

[35] D. Whittet, *Dust in the Galactic Environment*. Institute of Physics Publishing, UK, 2002.

[36] T. Armstrong, "LST, MST and SST Specifications." Private Communication, Feb 2021.

[37] D. King, "Atmospheric Extinction at the Roque de los Muchachos Observatory, La Palma," *RGO La Palma technical note no31*, 1985.

[38] F. Patat *et al.*, "Optical atmospheric extinction over Cerro Paranal," *A&A*, vol. 527, p. A91, 2011.

[39] C. Kitchin, *Astrophysical Techniques*. Adam Hilger Ltd, UK, 1984.

[40] *Optical SETI with Imaging Cherenkov Telescopes*, vol. 00, 2005.

[41] T. H. I.G. Hughes, *Measurements and their Uncertainties*. Oxford, UK, 2010.

[42] M. Ghigo *et al.*, "Ion figuring of large prototype mirror segments for the E-ELT," in *Advances in Optical and Mechanical Technologies for Telescopes and Instrumentation* (R. Navarro, C. R. Cunningham, and A. A. Barto, eds.), vol. 9151, pp. 225 – 236, International Society for Optics and Photonics, SPIE, 2014.

[43] G. Anglada-Escudé *et al.*, "A terrestrial planet candidate in a temperate orbit around Proxima Centauri," *Nature*, vol. 536, no. 7617, pp. 437–440, 2016.

[44] X. Bonfils *et al.*, "A temperate exo-Earth around a quiet M dwarf at 3.4 parsec," *A&A*, vol. 613, p. A25, 2018.

[45] S. Dreizler *et al.*, "RedDots: a temperate 1.5 Earth-mass planet candidate in a compact multiterrestrial planet system around GJ 1061," *MNRAS*, vol. 493, no. 1, pp. 536–550, 2020.

[46] "SIMBAD Astronomical Database - CDS (Strasbourg)." URL: `http://simbad.u-strasbg.fr/simbad/`, last accessed Apr 2021.

[47] M. Zechmeister *et al.*, "The CARMENES search for exoplanets around M dwarfs. Two temperate Earth-mass planet candidates around Teegarden's Star," *A&A*, vol. 627, p. A49, 2019.

[48] A. Wandel and L. Tal-Or, "On the Habitability of Teegarden's Star Planets," *ApJ*, vol. 880, no. 2, p. L21, 2019.

[49] E. V. Quintana *et al.*, "An Earth-Sized Planet in the Habitable Zone of a Cool Star," *Science*, vol. 344, no. 6181, pp. 277–280, 2014.

[50] D. Guberman and R. Paoletti, "Silicon photomultipliers in Very High Energy gamma-ray astrophysics," *JINST*, vol. 15, no. 05, pp. C05039–C05039, 2020.

[51] D. Guberman and P. Colin, "Performance of the MAGIC telescopes under moonlight," *Astropart.Phys.*, no. 94, 2017.

[52] S. Griffin and VERITAS Collaboration, "VERITAS Observations under Bright Moonlight," in *34th International Cosmic Ray Conference (ICRC2015)*, vol. 34 of *International Cosmic Ray Conference*, p. 989, 2015.

[53] *Two Nearby Habitable Worlds? - Planetary Habitability Laboratory @ UPR Arecibo*. URL: `http://phl.upr.edu/press-releases/twonearbyhabitableworlds`, last accessed Mar 30, 2021.

[54] V. V. Grootel *et al.*, "Stellar Parameters for Trappist-1," *ApJ*, vol. 853, no. 1, p. 30, 2018.

[55] E. Costa *et al.*, "The Solar Neighborhood. XVI. Parallaxes from CTIOPI: Final Results from the 1.5 m Telescope Program," *AJ*, vol. 132, no. 3, pp. 1234–1247, 2006.

[56] A. J. Burgasser and E. E. Mamajek, "On the Age of the TRAPPIST-1 System," *ApJ*, vol. 845, no. 2, p. 110, 2017.

[57] J. G. Learned, S. Pakvasa, and A. Zee, "Galactic Neutrino Communication," *PhLB*, vol. 671, no. 1, pp. 15–19, 2009.

[58] Z. K. Silagadze, "SETI and Muon Collider," *Acta Phys.Polon.*, no. B39, pp. 2943–2948, 2008. arXiv:0803.0409.

[59] J. M. Pasachoff and M. L. Kutner, "Neutrinos for Interstellar Communication," *CosSe*, vol. 1, no. 3, 1979.

[60] M. Subotowicz, "Interstellar communication by neutrino beams," *AcA*, vol. 6, 1979.

[61] P. Huber, "SubMarine Neutrino Communication," *PhLB*, vol. 692, no. 4, pp. 268–271, 2010.

[62] A. Siraj and A. Loeb, "The Copernican Principle Rules Out BLC1 as a Technological Radio Signal from the Alpha Centauri System," *arXiv pre-print*, 2021.

Acknowledgements

The author would like to thank Professor P. Chadwick for the invaluable advice and support she has provided over the past four years, as well as H. Petrovic, L. Van Schie, M. Black and T. Annal for their persistent enthusiasm, encouragement and kindness.